



HAL
open science

Super-quadratic upconversion luminescence among lanthanide ions

Irene Carrasco, L. Laversenne, Stefano Bigotta, Alessandra Toncelli, Mauro Tonelli, Alexander Zagumennyi, Markus Pollnau

► **To cite this version:**

Irene Carrasco, L. Laversenne, Stefano Bigotta, Alessandra Toncelli, Mauro Tonelli, et al.. Super-quadratic upconversion luminescence among lanthanide ions. *Optics Express*, 2019, 27 (23), pp.33217-33232. 10.1364/OE.27.033217. hal-02392501

HAL Id: hal-02392501

<https://hal.science/hal-02392501>

Submitted on 24 Aug 2023

HAL is a multi-disciplinary open access archive for the deposit and dissemination of scientific research documents, whether they are published or not. The documents may come from teaching and research institutions in France or abroad, or from public or private research centers.

L'archive ouverte pluridisciplinaire **HAL**, est destinée au dépôt et à la diffusion de documents scientifiques de niveau recherche, publiés ou non, émanant des établissements d'enseignement et de recherche français ou étrangers, des laboratoires publics ou privés.



Super-quadratic upconversion luminescence among lanthanide ions

IRENE CARRASCO,¹ LAETITIA LAVERSENNE,² STEFANO BIGOTTA,³
ALESSANDRA TONCELLI,³  MAURO TONELLI,³ ALEXANDER I.
ZAGUMENNYI,⁴  AND MARKUS POLLNAU^{1,*}

¹Advanced Technology Institute, Department of Electrical and Electronic Engineering, University of Surrey, Guildford GU2 7XH, United Kingdom

²Université Grenoble Alpes, CNRS, Grenoble INP, Institut Néel, 38000 Grenoble, France

³NEST-Istituto Nanoscienze-CNR and Dipartimento di Fisica, Università di Pisa, Largo B. Pontecorvo, 3, I-56127 Pisa, Italy

⁴Prokhorov Institute of General Physics, Russian Academy of Sciences, Vavilov Street 38, Moscow 119991, Russia

*m.pollnau@surrey.ac.uk

Abstract: We explore the arguably most fundamental aspect of energy-transfer upconversion (ETU), namely the dependence of upconversion luminescence from a higher-energy level, following ETU excitation from a metastable lower-energy level, on direct luminescence from that metastable level. We investigate ETU among neighboring Nd^{3+} ions in single crystals of GdVO_4 and $\text{LaSc}_3(\text{BO}_3)_4$ with different doping concentrations by measuring, after short-pulse laser excitation with different pump energies, the infrared luminescence decay from the metastable $^4\text{F}_{3/2}$ level and the yellow upconversion luminescence decay from the $^4\text{G}_{7/2}$ level. We observe a highly super-quadratic dependence of upconversion on direct luminescence intensity. We conclude that the commonly assumed quadratic law of ETU, as proposed by Grant's model and frequently employed in rate-equation simulations, is inadequate to the description of ETU processes. Whereas Zubenko's model, which considers a finite migration rate, provides significantly better fits to the experimental luminescence-decay curves, also this model cannot accurately reproduce the measured decay curves, partly because it does not take the non-homogeneous distribution of active ions into account.

© 2019 Optical Society of America under the terms of the [OSA Open Access Publishing Agreement](#)

1. Introduction

Energy transfer between optically active ions is a process in which an excited donor ion transfers all or part of its excitation energy to a neighboring acceptor ion, thereby promoting the acceptor ion to an excited state. Potential transfer mechanisms include multipole-multipole interaction and the exchange mechanism, the latter requiring a direct overlap of atomic functions that occurs only at extremely short distances. The most common interaction mechanism is electric dipole-dipole interaction. The probability of energy transfer depends on the availability of the excited donor ion, the acceptor ion, the energetic overlap between the involved electronic transitions, and the distance between the two ions [1].

Energy-transfer upconversion (ETU) [2–4] is an energy-transfer process in which the excited donor ion transfers all or part of its excitation energy to an already excited acceptor ion, thereby promoting it to a higher excited state. Inokuti and Hirayama [5] presented a treatment of the relationship between transfer rate and luminescence decay that has been adapted by a number of authors; see, e.g., [6]. It assumes that only donor-acceptor energy transfer occurs, whereas donor-donor transfer is negligible. In contrast, the model introduced by Grant [7] assumes that donor-donor transfer, which leads to energy migration within level i , i.e., energy transfer from an excited ion to a neighboring ion in its ground state, is infinitely fast, leading to the population

density N_i being equally distributed within the excitation volume. In Grant's model, if donor and acceptor ions are of the same type and both are initially in the same excited state i with its population density N_i , the transfer rate becomes a quadratic function of N_i , $R_{\text{ETU}} = W_{\text{ETU}} N_i^2$, where W_{ETU} is the macroscopic ETU parameter that quantifies the transfer probability. Due to its non-linear dependence on the population density N_i , the additional ETU rate leads to a non-exponential decay of the population density N_i and, hence, of luminescence from this level. Other models, such as those by Burshtein [8] and Zusman [9], neglect the quadratic dependence of the ETU process, thereby failing to predict the non-linear pump-power dependence of upconversion luminescence, but consider a finite migration time. Zubenko's model [10] combines the non-linear ETU rate of Grant's model with the finite migration rate of Zusman's model. All these models treat ETU based on the assumption that the environment is the same for all active ions. However, the ion distribution in a doped host material is usually non-uniform, in the best case statistical. Consequently, ETU introduces a spatial variation in the temporal emission characteristics and a macroscopic measurement of luminescence decay necessarily averages over this spatial variation.

Despite the very large number of investigations on the impact of ETU processes on infrared luminescence of rare-earth ions, see e.g. Refs. [10–14] for the case of Nd^{3+} , and the performance of infrared amplifiers and lasers, little attention has been paid to understanding the dynamics of the visible upconversion luminescence, see e.g. Refs. [15–17] for the case of Nd^{3+} , and its analysis is usually based on the commonly accepted assumption of a quadratic dependency of the visible upconversion on the direct infrared emission.

We tested the quadratic dependence of the ETU rate by performing a simple spectroscopic experiment. We measured the decay characteristics of luminescence emitted directly from the metastable electronic state of rare-earth ions doped into a crystalline host lattice and compared it with that of upconversion luminescence emitted from a short-lived, higher-energy electronic state following ETU from the metastable state. We find that the predicted quadratic dependence between upconversion and direct luminescence decay is strongly violated in the experiment. Whereas Grant's model delivers an exact quadratic dependence and cannot fit the measured luminescence-decay curves, Zubenko's model partially accounts for the non-quadratic nature.

2. Experimental

The spectroscopic systems investigated were single crystals of GdVO_4 and $\text{LaSc}_3(\text{BO}_3)_4$ doped with different concentrations of Nd^{3+} ions. GdVO_4 crystalizes in the $I4_1/amd$ space group. The Nd^{3+} ions enter the Gd^{3+} site, which has $42m$ point symmetry and is coordinated by 8 oxygen atoms. The number of sites available for Nd^{3+} doping in this material is $1.21 \times 10^{22} \text{ cm}^{-3}$ (equivalent to 100at.% doping). $\text{LaSc}_3(\text{BO}_3)_4$ belongs to the $R32$ space group. Within the structure, there are $5.1 \times 10^{21} \text{ cm}^{-3}$ La^{3+} sites available for Nd^{3+} doping (equivalent to 100at.% doping), with D_3 point symmetry and coordinated by tetragonal oxygen prisms. A remarkable feature of $\text{LaSc}_3(\text{BO}_3)_4$ is the large distance between nearest rare-earth neighbors of 0.59 nm [18,19,11]. In the case of GdVO_4 , samples with 1.3% ($1.57 \times 10^{-20} \text{ cm}^{-3}$), 2.8% ($3.39 \times 10^{-20} \text{ cm}^{-3}$), and 7.0% ($8.48 \times 10^{-20} \text{ cm}^{-3}$) Nd^{3+} concentration were selected, whereas for $\text{LaSc}_3(\text{BO}_3)_4$ crystals the Nd^{3+} concentrations were 10% ($5.1 \times 10^{-20} \text{ cm}^{-3}$), 25% ($1.28 \times 10^{-21} \text{ cm}^{-3}$), and 50% ($2.55 \times 10^{-21} \text{ cm}^{-3}$). The samples were grown at the General Physics Institute in Moscow, Russia, and the influence of ETU on the luminescence decay from the metastable ${}^4\text{F}_{3/2}$ state of Nd^{3+} was optically investigated in these samples in previous works [10,11].

The relevant excitation and relaxation processes are depicted in Fig. 1. Ground-state absorption (GSA) of pulsed laser light of ~ 30 ns duration and pulse energies varied between 0.08 and 1 mJ at wavelengths near 810 nm from a gain-switched extended-cavity Ti:Sapphire laser pumped by a flashlamp-pumped, Q -switched, frequency-doubled 532-nm laser excited the Nd^{3+} ions into the ${}^4\text{F}_{5/2}$ level. Fast non-radiative relaxation populated the Nd^{3+} ${}^4\text{F}_{3/2}$ metastable level

within the pump-pulse duration. From this level, several ETU processes led to the population of higher-energy excited states [12–14]. Under otherwise unchanged experimental conditions, luminescence-decay (LUM) curves were recorded by collecting either direct luminescence at the 1060-nm transition from the ${}^4F_{3/2}$ level or upconversion luminescence at the 590-nm transition from the short-lived ${}^4G_{7/2}$ upconversion level (upconversion luminescence at 530 nm was also monitored), passing the luminescence through a monochromator, and detecting the signal with a photomultiplier. The temporal resolution of the detection system was $\sim 2 \mu\text{s}$ for the infrared measurement and $\sim 0.5 \mu\text{s}$ when detecting the visible signal.

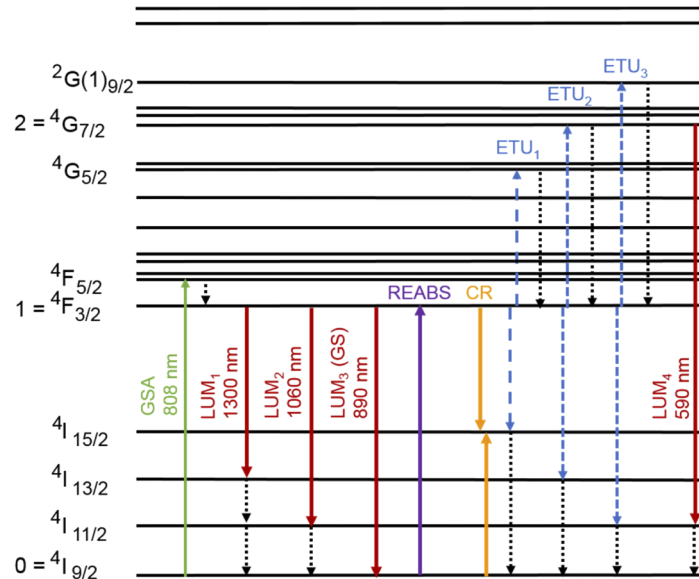


Fig. 1. Partial energy-level diagram of Nd^{3+} indicating the relevant spectroscopic processes: ground-state absorption (GSA), luminescence decay (LUM), reabsorption (REABS), cross relaxation (CR), energy-transfer upconversion (ETU), and multiphonon relaxation (dotted arrows). The levels considered for the simplified three-level scheme are numbered on the left-hand side.

Investigating Nd^{3+} ions in oxide crystal lattices has several distinct advantages. Firstly, various ETU transitions originating in the Nd^{3+} ${}^4F_{3/2}$ metastable electronic state possess strong transfer probabilities [11–14]. Secondly, the rather high values of the maximum phonon energies present in oxide host lattices ensure fast—typically a few ns [20]—non-radiative quenching of all except the ${}^4F_{3/2}$ excited electronic state. This feature enables us to investigate the relationship between direct and upconversion luminescence in an almost pure way, because the population density and, therefore, the luminescence intensity of the short-lived upconversion state reacts almost instantaneously to changes in the population density of the feeding metastable state. In addition, perturbation by excitation of the metastable or upconversion state from a third, longer-lived excited electronic state can be excluded. Finally, although quenched by fast non-radiative decay, several upconversion states of Nd^{3+} emit weak luminescence signals in the visible spectral region, most notably the yellow luminescence from the ${}^4G_{7/2}$ state, which allow us to probe their dynamics. As a result, the system can be described by a simplified three-level scheme as indicated in Fig. 1: the ${}^4I_{9/2}$ ground state (level 0), the ${}^4F_{3/2}$ metastable state (level 1), and the ${}^4G_{7/2}$ upconversion state (level 2). A complication is the occurrence of cross relaxation (CR) between two neighboring Nd^{3+} ions in their ${}^4F_{3/2}$ metastable excited and ${}^4I_{9/2}$ ground state, respectively, which shortens the ${}^4F_{3/2}$ luminescence-decay time owing to the additional relaxation path. On

the other hand, reabsorption (REABS) of the emitted ground-state luminescence by neighboring ions in their ground state can cause the measured decay time to be elongated compared to the intrinsic decay time of an isolated ion [21,22], particularly at the high dopant concentration present in the $\text{LaSc}_3(\text{BO}_3)_4$ samples.

Our interest in these two materials was evoked by the fact that, whilst donor-acceptor energy transfer (including ETU) in GdVO_4 is accelerated by migration of excitation within the $^4\text{F}_{3/2}$ metastable state, in $\text{LaSc}_3(\text{BO}_3)_4$ it takes place in the so-called static regime, i.e., the influence of migration on the occurrence of ETU is weak. The impact of this difference on the ETU processes in Nd^{3+} and, hence, on the dynamics of the infrared luminescence has previously been discussed [10,11].

The experimental consequence of choosing the above-described combination of energy-level system and host lattice is that significant pump energies are required to induce an ETU rate that is strong enough to sufficiently populate the short-lived upconversion levels to observe the faint upconversion luminescence. This, in turn, requires an extended pump-pulse duration to avoid ablation of the crystal surface by the short, intense pulse.

The measured decay curves of infrared luminescence at 1060 nm are presented in Fig. 2(a) for GdVO_4 and Fig. 3(a) for $\text{LaSc}_3(\text{BO}_3)_4$. For all six crystals, two different pump energies were tested, but changing the pump energy had no remarkable effect on the infrared decay

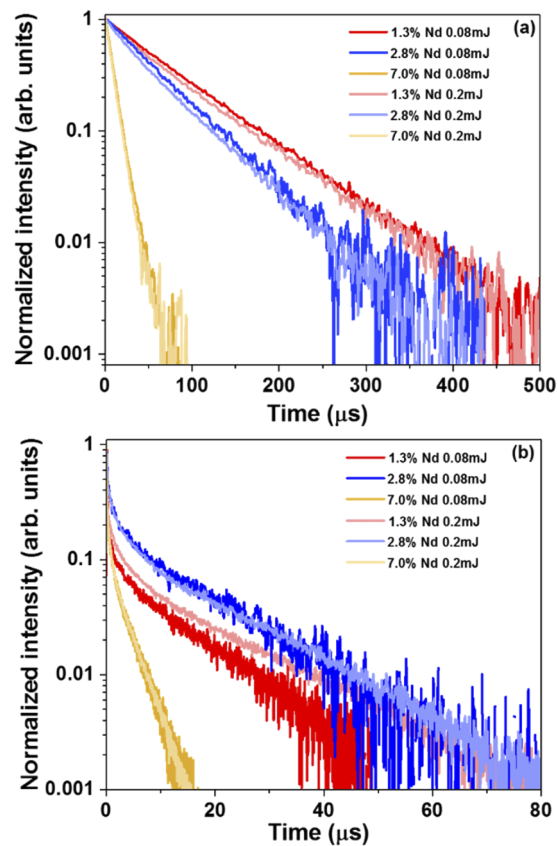


Fig. 2. Luminescence transients of (a) infrared luminescence from the $^4\text{F}_{3/2}$ level and (b) visible upconversion luminescence from the $^4\text{G}_{7/2}$ level of Nd^{3+} in GdVO_4 crystals with three different Nd^{3+} concentrations and two different pump energies.

curves. For both materials, the decay curves are non-exponential. In GdVO_4 , the decay time shortens significantly when the Nd^{3+} concentration is increased, even at the generally lower dopant concentrations investigated in GdVO_4 , evidencing the increase in nearest-neighbor Nd^{3+} ions, as well as enhanced energy migration, both increasing CR and ETU. On the contrary, in $\text{LaSc}_3(\text{BO}_3)_4$, for which energy migration is less relevant, the impact of increasing the dopant concentration is much smaller, and the decay time remains long even at the generally higher dopant concentrations investigated in $\text{LaSc}_3(\text{BO}_3)_4$. This concentration quenching dictated the choice of investigated dopant concentrations in the two materials, namely rather low Nd^{3+} concentrations in GdVO_4 versus rather high Nd^{3+} concentrations in $\text{LaSc}_3(\text{BO}_3)_4$.

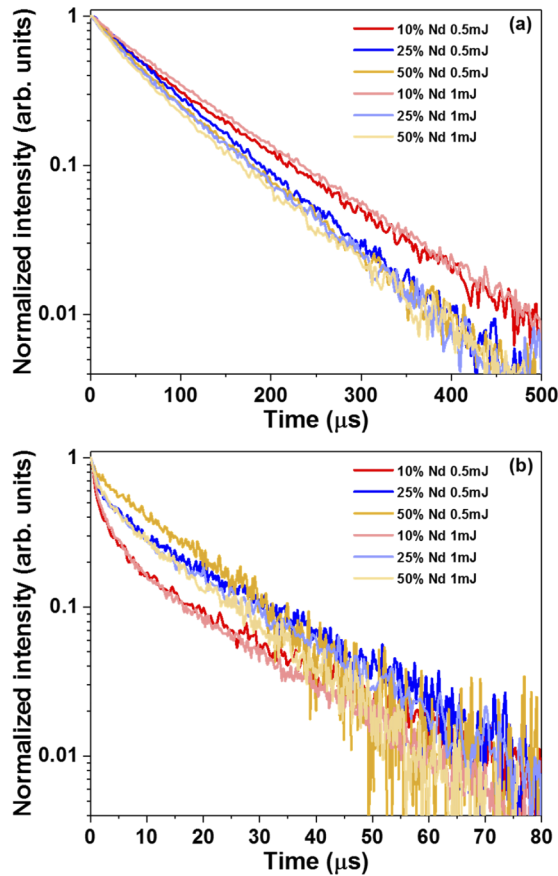


Fig. 3. Luminescence transients of (a) infrared luminescence from the ${}^4\text{F}_{3/2}$ level and (b) visible upconversion luminescence from the ${}^4\text{G}_{7/2}$ level of Nd^{3+} in $\text{LaSc}_3(\text{BO}_3)_4$ crystals with three different Nd^{3+} concentrations and two different pump energies.

The experimental decay curves of visible upconversion luminescence at 590 nm in GdVO_4 and $\text{LaSc}_3(\text{BO}_3)_4$ are presented in Fig. 2(b) and Fig. 3(b), respectively. The non-exponential behavior of these decay curves is more pronounced than for the infrared luminescence, with a very fast decay at short times followed by an almost exponential decay at long times. For GdVO_4 , comparison between the two samples with lower dopant concentrations indicates that the initial fast decay shortens as the Nd^{3+} content is increased. This effect is difficult to identify in the sample with the highest dopant concentration, because for this sample, as expected from the infrared decay curves, the upconversion luminescence decay is generally significantly shortened.

Like for the infrared emission, no remarkable change is observed when the pump energy is increased. Shortening of the initial fast decay with increasing Nd^{3+} concentration is also observed in $\text{LaSc}_3(\text{BO}_3)_4$. The time constant of the almost exponential tail is about 17 – 20 μs for all samples, except for the 7.0% Nd^{3+} -doped GdVO_4 sample where it amounts to approximately 3 μs .

3. Rate-equation model

As indicated in Section 2, various processes must be considered in the model to describe our system: GSA of pump energy, infrared LUM, REABS, CR, ETU, and upconversion LUM.

Although donor-acceptor energy-transfer models were initially intended to describe processes between non-equivalent ions, namely a donor in an excited state and an acceptor in its ground state, they have been widely applied to describe also upconversion processes between two excited ions [8,9]. This, however, does not eliminate the problem that most of the models assume linear quenching processes, which fundamentally deprive them of the capability of describing the nonlinear character of ETU.

To address this problem, Grant [7] proposed a model where a nonlinear rate equation is derived from first principles and an ETU process is taken into account via the rate

$$R_{ETU} = 2W_{ETU}N_1^2(t), \quad (1)$$

where W_{ETU} is the macroscopic ETU parameter, $N_1(t)$ is the time-dependent population density of the state in which the ETU process originates, and the “two-ion” character of ETU is expressed by the exponent of 2. However, even though this model allows to address the nonlinearity of the ETU process, it fails to describe effects caused by the finite time of energy migration, since it is based on the assumption that the migration rate is infinitely fast. To overcome this issue, Zubenko [10] proposed a model that relies on the same nonlinearity as described by Grant but considers a finite rate for the energy migration as introduced in Zusman’s model [9]. To do so, Zubenko assumed that the W_{ETU} coefficient in Grant’s equations can be directly replaced by Zusman’s nonlinear quenching rate $F(t)$, which is given by [23]

$$F(t) = \frac{2\pi^2}{3} \sqrt{\frac{C_{DA}}{\tau_0}} \left[\sqrt{\frac{\tau_0}{\pi t}} \exp(-t/\tau_0) + \text{erf} \left(\sqrt{\frac{t}{\tau_0}} \right) \right]. \quad (2)$$

In Eq. (2), C_{DA} is the concentration-independent donor-acceptor transfer microparameter and τ_0 is the most probable migration time, given by

$$\tau_0 = \frac{1}{C_{DD}N_d^2}, \quad (3)$$

C_{DD} being the concentration-independent donor-donor transfer microparameter and N_d the dopant concentration. From these parameters the macroscopic ETU parameter is deduced as [10]

$$W_{ETU} = \frac{\pi^2}{3} \sqrt{\frac{C_{DA}}{\tau_0}} = \frac{\pi^2}{3} \sqrt{C_{DD}C_{DA}N_d}. \quad (4)$$

In the case of infinitely fast migration ($\tau_0 \rightarrow 0$) the nonlinear quenching rate becomes time independent and thereby Zubenko’s description reduces to Grant’s model, with

$$W_{ETU} = C_{ETU}N_d, \quad (5)$$

where C_{ETU} is the concentration-independent microscopic ETU parameter in the case of infinitely fast migration.

When assuming that the pump energy is low enough not to bleach the ground state, the influence of CR can be accounted for by considering the effective lifetime $\tau_{1,\text{eff}}$ of the ${}^4\text{F}_{3/2}$ level as a function of Nd^{3+} concentration [24],

$$\frac{1}{\tau_{1,\text{eff}}(N_d)} = \frac{1}{\tau_1} + W_{\text{CR}}N_d, \quad (6)$$

where τ_1 is the intrinsic lifetime of the excited level involved in CR and W_{CR} is the time-independent macroscopic CR parameter which is proportional to the dopant concentration,

$$W_{\text{CR}} = C_{\text{CR}}N_d. \quad (7)$$

By combining Eqs. (6) and (7) and adjusting the concentration-independent value of the microscopic CR parameter C_{CR} it is possible to fit the measured decay constants, as described by van Dalfsen *et al.* [24]. The values of the effective decay time as a function of Nd^{3+} concentration for $\text{LaSc}_3(\text{BO}_3)_4$ are available in the literature [11], whereas for GdVO_4 we have relied on the experimental values from the present work.

Finally, we considered the description proposed by Kühn *et al.* [25] to model the effect of REABS of ground-state luminescence,

$$R_{\text{REABS}} = \beta(960 \text{ nm}) \frac{\sigma_{\text{abs}}N_dN_1(t)}{\tau_1(\sigma N_d + \ell^{-1})}, \quad (8)$$

where σ_{abs} is the absorption cross section, ℓ is a reabsorption parameter, and the factor β (960 nm) ≈ 0.46 accounts for the branching ratio of the ${}^4\text{F}_{3/2} \rightarrow {}^4\text{I}_{9/2}$ ground-state transition [26].

Hence, the temporal dynamics of the excited-state population density of the metastable ${}^4\text{F}_{3/2}$ state can be described with the rate equation

$$\frac{dN_1(t)}{dt} = \frac{N_2(t)}{\tau_2} - 2fN_1^2(t) - \frac{N_1(t)}{\tau_1} - W_{\text{CR}}N_0(t)N_1(t) + \beta(960 \text{ nm}) \frac{\sigma_{\text{abs}}N_dN_1(t)}{\tau_1(\sigma N_d + \ell^{-1})}, \quad (9)$$

where $N_2(t)$ and τ_2 are the time-dependent population density and intrinsic lifetime of the upconversion level, respectively, and f quantifies the ETU process. For the calculation of Eq. (9) we consider τ_2 to be infinitely fast, hence $N_2/\tau_2 = fN_1^2(t)$. Furthermore, we assume that, for the upconversion states, multiphonon relaxation is fast compared to LUM_2 (590 nm), hence almost all upconverted ions return to the ${}^4\text{F}_{3/2}$ level. We consider a single upconversion process, using a single parameter f to describe the combined rate of ETU_1 , ETU_2 , and ETU_3 (Fig. 1), since it does not make any difference for the temporal shape of the upconversion decay curve whether either (a) all three ETU processes end up in the same level or in different ones, or (b) in which of the three levels the upconversion luminescence originates. The ground-state population density can be approximated by $N_0(t) = N_d - N_1(t)$, because the population density $N_2(t)$ of the upconversion states is negligible compared to N_0 and N_1 .

We evaluated three different situations to analyse the infrared decay curves, namely considering (i) only ETU, (ii) ETU and CR, and (iii) ETU, CR, and REABS. To describe the ETU process, both Grant's and Zubenko's models have been tested separately for these three situations, considering either $f = W_{\text{ETU}}$ from Eq. (5) or $f = F(t)$ from Eq. (2), respectively. For each of the six different combinations of model and situation we fitted the whole set of six experimental infrared decay curves independently for GdVO_4 and $\text{LaSc}_3(\text{BO}_3)_4$, with the parameters differing from one fit to the other. Where applicable, C_{ETU} (Grant's model) or C_{DA} and C_{DD} (Zubenko's model), and ℓ were used as free parameters. None of these parameters depends on the launched pump energy, i.e., the same values were employed for fitting the low- and high-pump-energy experimental decay curves. Of these parameters, only ℓ depends on the dopant concentration.

The rate equation for the temporal dynamics of the combined population densities of the upconversion states is given by

$$\frac{dN_2}{dt} = fN_1^2(t) - \frac{N_2(t)}{\tau_2}. \quad (10)$$

Since the lifetimes of the upconversion states are very short compared to the lifetime of the metastable state in which ETU originates, Eq. (10) can be solved in a quasi-steady state,

$$N_2(t) = \tau_2 f N_1^2(t). \quad (11)$$

Generally, the infrared and visible luminescence intensities I_{IR} and I_{VIS} are proportional to the excitation densities N_1 and N_2 , respectively. The actual value of τ_2 is, therefore, not relevant for fitting the measured upconversion-decay curves, because it becomes part of the proportionality constant between I_{VIS} and N_2 . To fit the visible decay curves we also considered both Grant's and Zubenko's approaches. The consequence of Grant's model is that the visible upconversion emission depends quadratically on the infrared luminescence, $I_{VIS} \propto I_{IR}^2$. On the other hand, by introducing a finite migration time, Zubenko's model modifies the relation between the visible upconversion and the infrared luminescence, and the more general dependence $I_{VIS} \propto R_{ETU}$ holds. In our model, we implemented Grant's description by considering that $I_{VIS} \text{ (simulated)} \propto (I_{IR} \text{ (simulated)})^2$, whereas for Zubenko's theory we have considered that $I_{VIS} \text{ (simulated)} \propto R_{ETU} \text{ (simulated)}$. Therefore, no additional free parameters are included to fit the upconversion-decay curves and, consequently, the model predictions for the visible luminescence decay are purely based on the infrared simulation. The parameters used in the calculations of luminescence-decay curves are presented in Table 1. The values of the intrinsic lifetime τ_1 were taken from [11]. We averaged the value of $\tau_1 = 1.15 \times 10^{-4}$ s for $\text{LaSc}_3(\text{BO}_3)_4$ from the values of 1.12×10^{-4} s for 0.1at.% and 1.18×10^{-4} s for 1, 3, and 10at.%. The values of the absorption cross sections were taken from [26]. The other parameters result from the fits with the models.

Table 1. Parameter values used in luminescence-decay calculations for GdVO₄ and LaSc₃(BO₃)₄ crystals

Model	Parameter	Symbol	Unit	GdVO ₄			LaSc ₃ (BO ₃) ₄		
				1.3%	2.8%	7.0%	10%	25%	50%
Both	Intrinsic lifetime	τ_1	10^{-4} s	0.97	0.97	0.97	1.15	1.15	1.15
	Absorption cross section	σ_{abs}	10^{-20} cm ²	51	51	51	1.9	1.9	1.9
	Cross-relaxation microparameter	C_{CR}	10^{-39} cm ⁶ /s	94	94	94	1.2	1.2	1.2
	Cross-relaxation macroparameter	W_{CR}	10^{-19} cm ³ /s	148	319	797	6.12	15.4	30.6
Grant	Upconversion microparameter	C_{ETU}	10^{-39} cm ⁶ /s	50	50	50	2	2	2
	Upconversion macroparameter	W_{ETU}	10^{-19} cm ³ /s	75.8	117	424	10.2	25.6	51.0
	Reabsorption parameter	ℓ	10^{-4} cm	1	200	1	10	1	3000
Zubenko	Most probable migration time	τ_0	10^{-6} s	20300	4350	695	48.1	7.63	1.92
	Donor-donor microparameter	C_{DD}	10^{-39} cm ⁶ /s	2	2	2	80	80	80
	Donor-acceptor microparameter	C_{DA}	10^{-42} cm ⁶ /s	90	90	90	6	6	6
	Upconversion macroparameter	W_{ETU}	10^{-19} cm ³ /s	2.19	4.73	11.8	11.6	29.2	58.1
	Reabsorption parameter	ℓ	10^{-4} cm	1	50	1	1	4	6

4. Infrared luminescence

Figure 4 presents the measured effective luminescence-decay time of the $^4F_{3/2}$ level in GdVO₄ and LaSc₃(BO₃)₄, together with the calculated fit (obtained as described in Section 3) for optimized

values of the CR micro-parameter of $C_{CR} = 9.4 \times 10^{-38} \text{ cm}^6 \text{ s}^{-1}$ and $C_{CR} = 1.2 \times 10^{-39} \text{ cm}^6 \text{ s}^{-1}$, respectively. As a consequence of the shorter nearest-neighbor distance present in GdVO_4 , the cross relaxation among Nd^{3+} ions is already significant at low Nd^{3+} concentrations, whereas in $\text{LaSc}_3(\text{BO}_3)_4$ it becomes relevant only for relatively high dopant concentrations. Consequently, the C_{CR} value is almost two orders of magnitude higher in GdVO_4 .

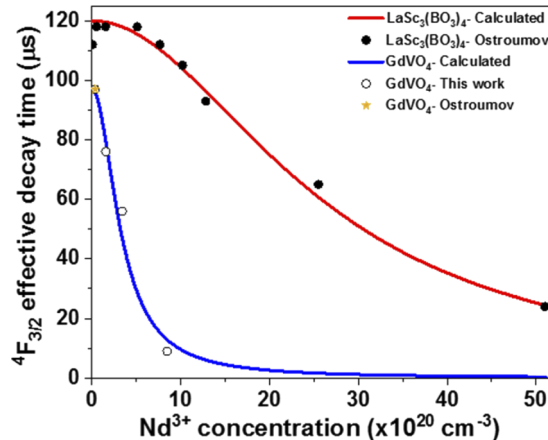


Fig. 4. Effective luminescence-decay time measured in $\text{LaSc}_3(\text{BO}_3)_4$ (black circles [11]) and GdVO_4 (white circles [present work]; yellow star [11]) as a function of Nd^{3+} concentration. The corresponding fits calculated according to Eqs. (6) and (7) are also included (red line for $\text{LaSc}_3(\text{BO}_3)_4$, blue line for GdVO_4).

Figure 5 presents the experimental infrared luminescence-decay curves, measured for pump energies of 0.08 mJ in GdVO_4 and 0.5 mJ in $\text{LaSc}_3(\text{BO}_3)_4$, compared with the simulated luminescence-decay curves obtained using Grant's and Zubenko's models. As indicated in Section 3, we investigated three different situations depending on the processes considered: (i) only ETU, (ii) ETU and CR, and (iii) ETU, CR, and REABS. In the case of GdVO_4 , as expected because of the strong influence of CR in this host, the model is not able to reproduce the experimental results if only ETU is considered (Fig. 5(a)), predicting not only a much slower decay but also a profile for the decay curves that is substantially different from the ones observed experimentally. By considering also CR (Fig. 5(b)), the fit improves noticeably, and the simulation can reproduce the shortening of the decay time as the Nd^{3+} concentration is increased, as well as to predict a much better profile. The further inclusion of REABS (Fig. 5(c)) allows us to correct the deviation observed for model (ii) in the decay curve corresponding to the 2.8% sample. However, for the 7.0% sample, neither model provides an accurate fit. The decay curves obtained when considering Grant's or Zubenko's model do not differ significantly, except when only ETU is considered. In this case, Grant's model predicts a slightly slower decay than Zubenko's.

For $\text{LaSc}_3(\text{BO}_3)_4$, the decay curves obtained considering only ETU (Fig. 5(d)) deviate less from the experimental decay curves than in the case of GdVO_4 , although again the profile deviates from the experimental result. Taking also CR into account (Fig. 5(e)) provides a better profile and, for the 10%- and the 25%-doped samples, the model predicts reasonably well the experimental decay curves. However, for the 50% Nd^{3+} sample the experimentally observed decay is slower than predicted. Including REABS (Fig. 5(f)) compensates the effect of CR and provides a better fit. However, as for GdVO_4 , none of the assumptions accurately reproduces the experimental decay curve of the sample with the highest doping level. In the case of $\text{LaSc}_3(\text{BO}_3)_4$, the simulated decay curves obtained with Grant's and Zubenko's models are practically indistinguishable.

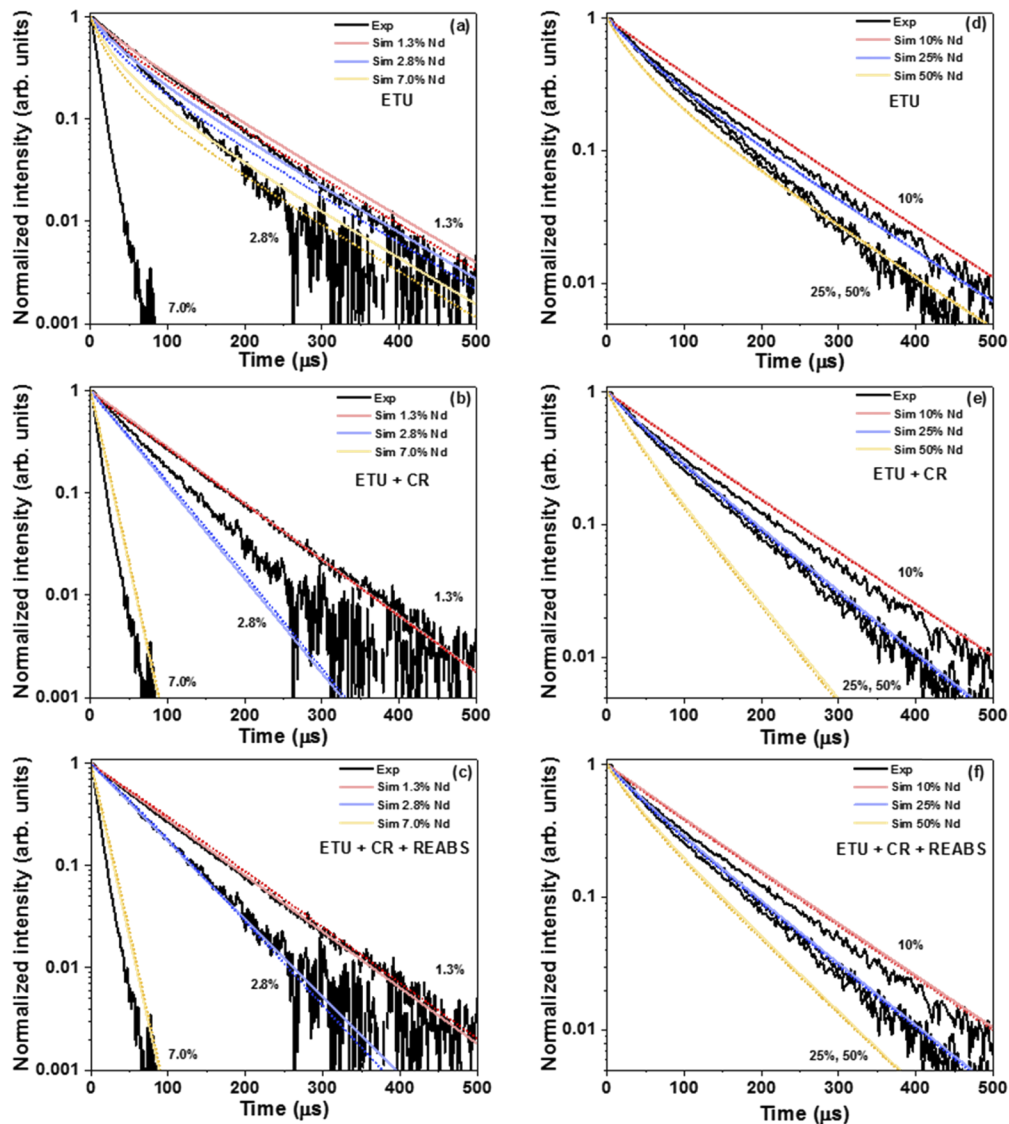


Fig. 5. Measured infrared luminescence-decay curves from the ${}^4F_{3/2}$ level of Nd^{3+} for the three different Nd^{3+} concentrations and pump energies of (a – c) 0.08 mJ in GdVO_4 and (d – f) 0.5 mJ in $\text{LaSc}_3(\text{BO}_3)_4$, compared with fits when sequentially including the following processes in the model: (a, d) ETU, (b, e) ETU and CR, and (c, f) ETU, CR, and REABS. The simulated curves calculated with Grant's model are shown as solid lines, whereas those corresponding to Zubenko's model are shown as dotted lines.

Without doubt, the REABS process influences the population dynamics of Nd^{3+} ions. As described in Section 3, the model proposed by Kühn *et al.* [25] allows us to include reabsorption in our rate-equation model via a term that considers only one free parameter, ℓ , which accounts for the mean path length a photon propagates after being initially emitted and then—potentially multiple times—being re-absorbed and re-emitted again before leaving the crystal. The probability of a photon to be re-absorbed is described by this distance. Since increasing the number of optically active centers increases the probability of the photon being re-absorbed and re-emitted

away from the crystal edge, which increases the distance the photon travels inside the crystal, one should expect ℓ to increase with increasing dopant concentration. Therefore, we considered ℓ as a concentration-dependent parameter in our simulations, but without defining a particular dependence, i.e., ℓ is treated as a free parameter. In the case of $\text{LaSc}_3(\text{BO}_3)_4$ the obtained values follow reasonably well the expected behavior, whereas no clear trend is found in the case of GdVO_4 .

Since the best fits of the infrared luminescence-decay curves are obtained when considering ETU, CR, and REABS, we will investigate the upconversion luminescence-decay curves by including all three processes.

5. Upconversion luminescence

Figure 6 presents the experimental and fitted curves of infrared decay from the $^4\text{F}_{3/2}$ level and visible decay from the $^4\text{G}_{7/2}$ level for three different Nd^{3+} concentrations in GdVO_4 measured at low pump energy of 0.08 mJ (Figs. 6(a)–6(c)) and high pump energy of 0.2 mJ (Figs. 6(d)–6(f)), when including the ETU, CR, and REABS processes. Most striking is the obvious deviation of the experimental visible upconversion luminescence decay (grey curve) from the quadratic law predicted by Grant's model (red dotted curve). The dependence of visible upconversion on infrared direct luminescence is close to a power-to-the-four dependence.

As observed previously in Fig. 5(c), the infrared fit using either Zubenko's or Grant's model and including ETU, CR, and REABS is good for decay curves with lower pump energy. However, it deviates significantly for the sample with the highest dopant concentration, independently of the applied pump energy. Moreover, for high pump energy the simulation describes a positive bending, particularly when Zubenko's model is employed, possibly resulting from an overestimation of the cross relaxation. The situation for the visible decay curves is entirely different. Grant's model fails to describe the visible decay curves for all Nd^{3+} concentrations and pump energies. The visible simulated decay curves obtained using Zubenko's model provide a better fit of the experimental data and clearly exhibit a super-quadratic dependence on infrared luminescence decay, even though the agreement is not perfect, especially for the 7.0% sample measured at high pump energy. Zubenko's model allows to describe reasonably well the overall profile of the decay curves, including the fast initial decay and the slightly slower tail at longer times.

The results are similar for $\text{LaSc}_3(\text{BO}_3)_4$ for 0.5 mJ of pump energy (Figs. 7(a)–7(c)) and 1 mJ of pump energy (Figs. 7(d)–7(f)). Again, most striking is the obvious deviation of the visible upconversion luminescence decay (grey curve) from the quadratic law predicted by Grant's model (red dotted curve).

Also for $\text{LaSc}_3(\text{BO}_3)_4$, both Grant's and Zubenko's models provide a reasonably good fit of the infrared decay curves, slightly better for the decay curves measured under low pump energy, except for the 50% Nd^{3+} sample, which is not well fitted independently of the value of the pump energy. Regarding the visible decay curves, the better description is, again, obtained when Zubenko's model is considered, whereas Grant's description provides incorrect results. However, for $\text{LaSc}_3(\text{BO}_3)_4$ the simulated decay curves obtained with Zubenko's approach do not provide a fit as good as in the case of GdVO_4 , neither for low nor for high pump energy. The model predicts a faster initial decay, particularly for the 25% and 50% Nd^{3+} samples, and a longer tail at long times than observed in the experiment. The fact that in Fig. 7(f) the visible decay curve seems to be reasonably well fitted must be accidental, since the fit of the infrared decay curve is not adequate and the visible luminescence is directly linked to the infrared one.

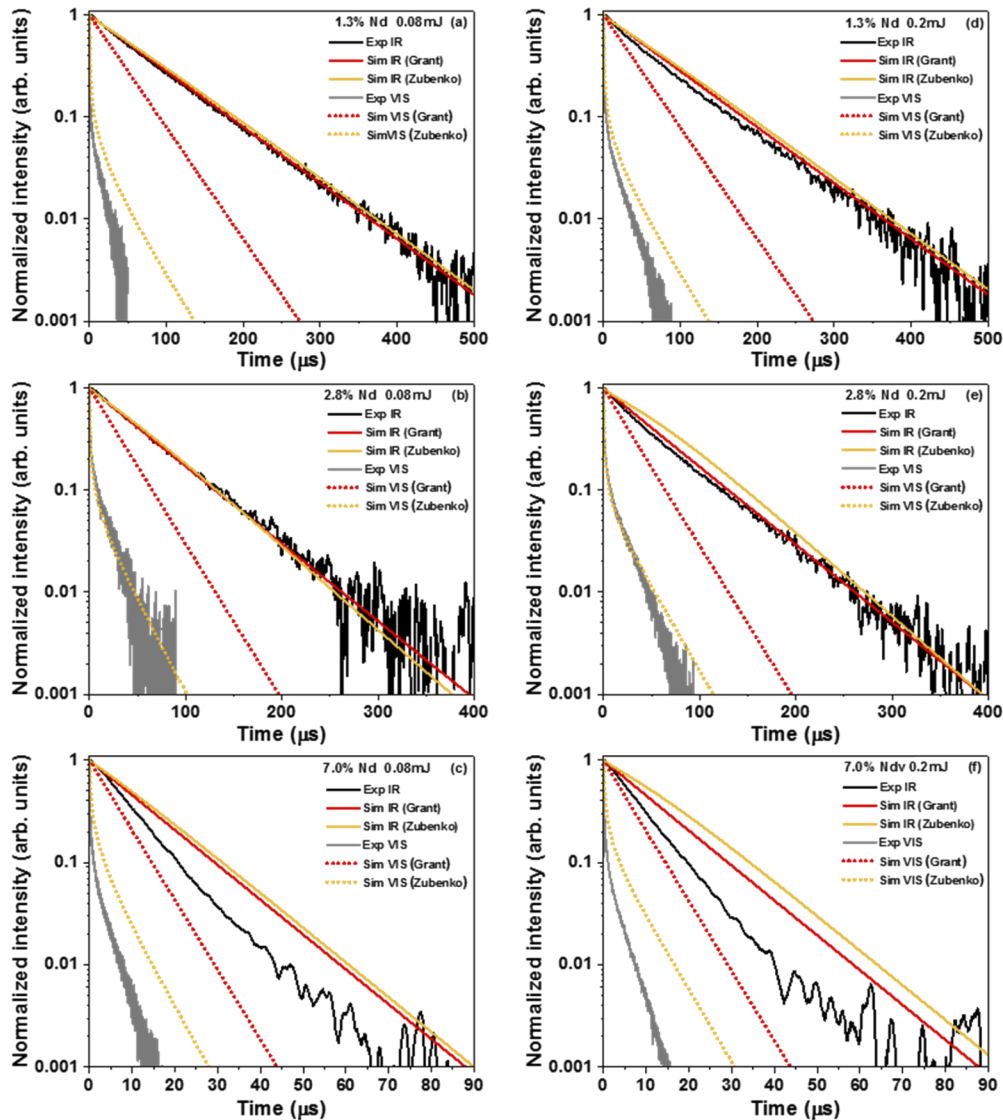


Fig. 6. Measured infrared (black) and visible (grey) luminescence-decay curves from the ${}^4F_{3/2}$ and ${}^4G_{7/2}$ levels, respectively, in $GdVO_4$ for low pump energy of 0.08 mJ (a – c) and high pump energy of 0.2 mJ (d – f) and for (a, d) low, (b, e) medium, and (d, f) high dopant concentration, compared with fits using Grant's and Zubenko's models including ETU, CR, and REABS. The simulated decay curves obtained using Grant's model are shown in red, whereas the ones obtained with Zubenko's model are shown in yellow. For both models the solid curves correspond to the infrared and the dotted ones to the visible luminescence.

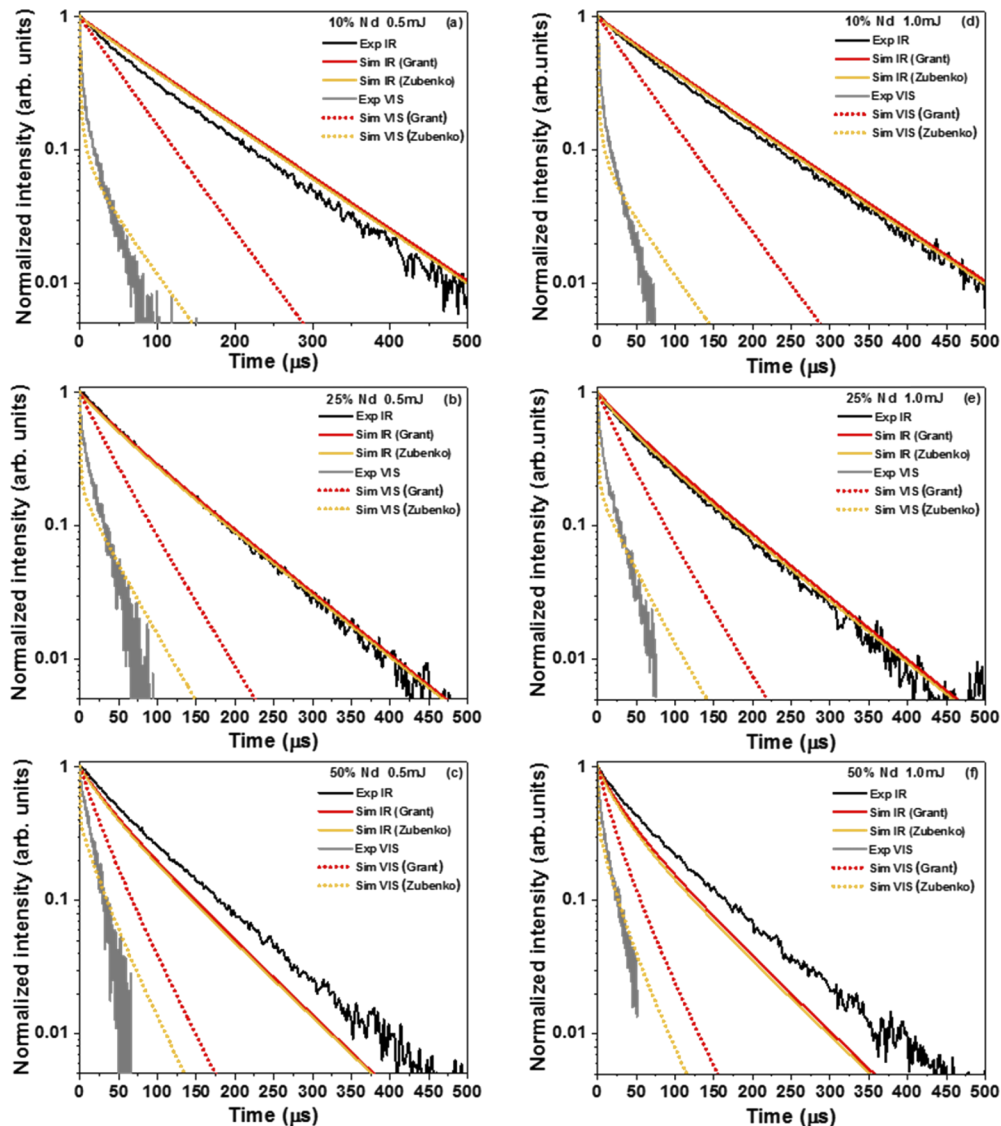


Fig. 7. Measured infrared (black) and visible (grey) luminescence-decay curves from the ${}^4F_{3/2}$ and ${}^4G_{7/2}$ levels, respectively, in $\text{LaSc}_3(\text{BO}_3)_4$ for low pump energy of 0.5 mJ (a – c) and high pump energy of 1 mJ (d – f) and for (a, d) low, (b, e) medium, and (d, f) high dopant concentration, compared with fits using Grant’s and Zubenko’s models including ETU, CR, and REABS. The simulated decay curves obtained using Grant’s model are shown in red, whereas the ones obtained with Zubenko’s model are shown in yellow. For both models the solid curves correspond to the infrared and the dotted ones to the visible luminescence.

6. Discussion

In both investigated materials, the calculated infrared luminescence-decay curves fit the experimental data reasonably well. Even though the agreement with the measured decay curves is not perfect, the simulations allow to reproduce the general behavior and profile. This is true for both Grant’s and Zubenko’s models, because the difference between the two is limited to describing ETU, whereas the temporal shapes of the infrared decay curves are significantly influenced

by CR. However, the difference between the two models in the description of ETU becomes highly evident when the visible decay curves are analyzed. From Figs. 6 and 7 it becomes clear that Grant's model is unable to explain the visible decay curves for any of the studied crystals, independently of whether the ETU takes place in the "static" or "migration-accelerated" regime. The widely accepted quadratic dependence of visible upconversion on infrared luminescence intensity does not withstand our experimental scrutiny. Zubenko's model also considers a quadratic dependence of visible on infrared emission but modifies the temporal shape via the finite migration time, resulting in a time-dependent nonlinear quenching rate. As can be observed from Figs. 6 and 7, even though for the infrared emission this model provides similar results as Grant's model, Zubenko's approach provides a significantly better description of the visible decay curves and, particularly, predicts a super-quadratic dependence of upconversion on direct luminescence decay.

However, the fits are still far from being perfect. We suspect that the discrepancy is, at least partly, due to the fact that, like Grant's and most other models, Zubenko's model treats all ions equally, thereby neglecting the non-homogeneous distribution of active ions. The information contained in the upconversion luminescence distinguishes itself from that contained in the direct luminescence, because it results only from those ions that have active neighbors and can, therefore, undergo ETU, whereas the direct luminescence contains information from all active ions.

Several models of energy-transfer processes in RE³⁺-doped materials based on a statistical description of the nearest-neighbor shell have been developed [23,27–33]. Such models often require knowledge of the exact crystallographic structure of the material [27,28]. Some models use a fully statistical approach by considering a large number of possible donor-acceptor environments [29–32]. However, due to the complexity of such derivations, normally only simplified energy-transfer mechanisms can be described. For systems exhibiting several energy-transfer processes and an extended energy-level system, the rate-equation formalism is simpler and can be directly applied to fitting the experimentally observable pump-, concentration-, and time-dependent luminescence intensities.

We have extended the rate-equation formalism by assuming a simple set of distinct ion classes [23,33]. This approach is straight forward and accurate when a fraction of ions exhibits fast luminescence quenching [23], such that these ions are mostly in the ground state. However, when trying to distinguish two ion classes that both contribute to luminescence, e.g. one without active neighbors that is excluded from ETU and another with active neighbors that participates in ETU [33], the situation is less clear, as these two ion classes might nevertheless communicate with each other via energy migration and luminescence reabsorption. Consequently, it would be impossible to apply two distinct sets of rate equations to the two ion classes. In case the two ion classes do not communicate with each other, then also energy migration within the class of ions that contributes to ETU may well be partially inhibited. Consequently, only static upconversion could occur when an ion has only one nearest-neighbor active ion, whereas a short-range energy migration could occur in clusters comprising several ions. In such a case, the usual rate-equation formalism, e.g. Grant's or Zubenko's model, would not even apply within this ion class. It becomes clear from these considerations that a rate-equation formalism is always a compromise, and sometimes a rather coarse one.

7. Summary

The present investigation has underlined the following points. (i) It is insufficient to measure only the luminescence-decay curves of luminescence that directly emerges from an excited level that exhibits ETU. The upconversion luminescence contains important additional information. (ii) The experimental dependence of upconversion on direct luminescence is highly super-quadratic. (iii) The quadratic law of ETU as proposed by Grant's model is merely a fairy tale. (iv) Zubenko's model, which includes a finite migration rate resulting in a time-dependent nonlinear quenching

rate, is significantly closer to the experimental reality, but its fits are also far from being excellent. Hence, also Zubenko's model is hardly adequate to the description of ETU, quite probably because it treats all ions equally, thereby neglecting the influence of an inhomogeneous ion distribution. At this point, it is not obvious how to establish a model that can accurately describe ETU.

Funding

European Research Council (No. 341206).

Acknowledgments

I.C. and M.P. acknowledge financial support by the European Research Council (ERC) Advanced Grant "Optical Ultra-Sensor" No. 341206. The authors thank Willy Lüthy from the University of Bern for helpful discussions.

References

1. D. L. Dexter, "A theory of sensitized luminescence in solids," *J. Chem. Phys.* **21**(5), 836–850 (1953).
2. F. Auzel, "Materials and devices using double-pumped phosphors with energy transfer," *Proc. IEEE* **61**(6), 758–786 (1973).
3. J. C. Wright, "Up-conversion and excited state energy transfer in rare-earth doped materials," in *Topics in Applied Physics: Radiationless Processes in Molecules and Condensed Phases*, Vol. 15, F. K. Fong, ed. (Springer, Berlin, 1976), pp. 239–295.
4. F. Auzel, "Upconversion and anti-Stokes processes with f and d ions in solids," *Chem. Rev.* **104**(1), 139–174 (2004).
5. M. Inokuti and F. Hirayama, "Influence of energy transfer by the exchange mechanism on donor luminescence," *J. Chem. Phys.* **43**(6), 1978–1989 (1965).
6. P. Villanueva-Delgado, K. W. Krämer, R. Valiente, M. de Jong, and A. Meijerink, "Modeling blue to UV upconversion in β -NaYF₄:Tm³⁺," *Phys. Chem. Chem. Phys.* **18**(39), 27396–27404 (2016).
7. W. J. C. Grant, "Role of rate equations in the theory of luminescent energy transfer," *Phys. Rev. B* **4**(2), 648–663 (1971).
8. A. I. Burshtein, "The concentration quenching of non-coherent excitations in solutions," *Usp. Fiz. Nauk* **143**(4), 553–600 (1984). [Engl. transl.: *Sov. Phys. Usp.* **27**(8), 579–606 (1984).]
9. L. D. Zusman, "Kinetics of luminescence damping in the hopping mechanism of quenching," *Sov. Phys. JETP* **46**(2), 347–351 (1977).
10. D. A. Zubenko, M. A. Noginov, V. A. Smirnov, and I. A. Shcherbakov, "Different mechanisms of nonlinear quenching of luminescence," *Phys. Rev. B* **55**(14), 8881–8886 (1997).
11. V. Ostroumov, T. Jensen, J. P. Meyn, G. Huber, and M. A. Noginov, "Study of luminescence concentration quenching and energy transfer upconversion in Nd-doped LaSc₃(BO₃)₄ and GdVO₄," *J. Opt. Soc. Am. B* **15**(3), 1052–1060 (1998).
12. Y. Guyot, H. Manaa, J. Y. Rivoire, R. Moncorgé, N. Garnier, E. Descroix, M. Bon, and P. Laporte, "Excited-state-absorption and up-conversion studies of Nd³⁺-doped-single crystals Y₃Al₅O₁₂, YLiF₄, and LaMgAl₁₁O₁₉," *Phys. Rev. B* **51**(2), 784–799 (1995).
13. M. Pollnau, P. J. Hardman, W. A. Clarkson, and D. C. Hanna, "Upconversion, lifetime quenching, and ground-state bleaching in Nd³⁺:LiYF₄," *Opt. Commun.* **147**(1-3), 203–211 (1998).
14. M. Pollnau, P. J. Hardman, M. A. Kern, W. A. Clarkson, and D. C. Hanna, "Upconversion-induced heat generation and thermal lensing in Nd:YLF and Nd:YAG," *Phys. Rev. B* **58**(24), 16076–16092 (1998).
15. T. Chuang and H. R. Verdún, "Energy transfer up-conversion and excited state absorption of laser radiation in Nd:YLF laser crystals," *IEEE J. Quantum Electron.* **32**(1), 79–91 (1996).
16. J. D. Zuegel and W. Seka, "Upconversion and reduced ⁴F_{3/2} upper-state lifetime in intensely pumped Nd:YLF," *Appl. Opt.* **38**(12), 2714–2723 (1999).
17. M. Malinowski, B. Jacquier, M. Bouazaoui, M. F. Joubert, and C. Linares, "Laser-induced fluorescence and up-conversion processes in LiYF₄:Nd³⁺ laser crystals," *Phys. Rev. B* **41**(1), 31–40 (1990).
18. H. Y. P. Hong and K. Dwight, "Crystal structure and fluorescence lifetime of NdAl₃(BO₃)₄, a promising laser material," *Mater. Res. Bull.* **9**(12), 1661–1665 (1974).
19. V. A. Dotsenko and N. P. Efrushina, "Static energy transfer in YAl₃B₄O₁₂:Ln³⁺ (Ln³⁺ = Sm³⁺, Dy³⁺)," *Phys. Stat. Sol. A* **130**(1), 199–205 (1992).
20. C. Bibeau, S. A. Payne, and H. T. Powell, "Direct measurements of the terminal laser level lifetime in neodymium-doped crystals and glasses," *J. Opt. Soc. Am. B* **12**(10), 1981–1992 (1995).
21. D. S. Sumida and T. Y. Fan, "Effect of radiation trapping on fluorescence lifetime and emission cross section measurements in solid-state laser media," *Opt. Lett.* **19**(17), 1343–1345 (1994).

22. Y. S. Yong, S. Aravazhi, S. A. Vázquez-Córdova, J. J. Carvajal, F. Díaz, J. L. Herek, S. M. García-Blanco, and M. Pollnau, "Direct confocal lifetime measurements on rare-earth-doped media exhibiting radiation trapping," *Opt. Mater. Express* **7**(2), 527–532 (2017).
23. L. Agazzi, K. Wörhoff, and M. Pollnau, "Energy-transfer-upconversion models, their applicability and breakdown in the presence of spectroscopically distinct ion classes: A case study in amorphous $\text{Al}_2\text{O}_3:\text{Er}^{3+}$," *J. Phys. Chem. C* **117**(13), 6759–6776 (2013).
24. K. van Dalfsen, S. Aravazhi, C. Grivas, S. M. García-Blanco, and M. Pollnau, "Thulium channel waveguide laser with 1.6 W of output power and ~80% slope efficiency," *Opt. Lett.* **39**(15), 4380–4383 (2014).
25. H. Kühn, S. T. Friedrich-Thornton, C. Kränkel, R. Peters, and K. Petermann, "Model for the calculation of radiation trapping and description of the pinhole method," *Opt. Lett.* **32**(13), 1908–1910 (2007).
26. J. P. Meyn, T. Jensen, and G. Huber, "Spectroscopic properties and efficient diode-pumped laser operation of neodymium-doped lanthanum scandium borate," *IEEE J. Quantum Electron.* **30**(4), 913–917 (1994).
27. H. Siebold and J. Heber, "'Discrete shell model' for analysing time-resolved energy transfer in solids," *J. Lumin.* **22**(3), 297–319 (1981).
28. S. O. Vasquez and C. D. Flint, "A shell model for cross relaxation in elpasolite crystals: application to the $^3\text{P}_0$ and $^1\text{G}_4$ states of $\text{Cs}_2\text{NaY}_{1-x}\text{Pr}_x\text{Cl}_6$," *Chem. Phys. Lett.* **238**(4-6), 378–386 (1995).
29. C. Z. Hadad and S. O. Vasquez, "Statistical approach to the transient up-converted population in monodoped amorphous solids," *Phys. Chem. Chem. Phys.* **5**(14), 3027–3033 (2003).
30. F. T. Rabouw, S. A. den Hartog, T. Senden, and A. Meijerink, "Photonic effects on the Förster resonance energy transfer efficiency," *Nat. Commun.* **5**(1), 3610 (2014).
31. D. C. Yu, F. T. Rabouw, W. Q. Boon, T. Kieboom, S. Ye, Q. Y. Zhang, and A. Meijerink, "Insights into the energy transfer mechanism in Ce^{3+} - Yb^{3+} codoped YAG phosphors," *Phys. Rev. B* **90**(16), 165126 (2014).
32. F. T. Rabouw and A. Meijerink, "Modeling the cooperative energy transfer dynamics of quantum cutting for solar cells," *J. Phys. Chem. C* **119**(5), 2364–2370 (2015).
33. P. Loiko and M. Pollnau, "Stochastic model of energy-transfer processes among rare-earth ions. Example of $\text{Al}_2\text{O}_3:\text{Tm}^{3+}$," *J. Phys. Chem. C* **120**(46), 26480–26489 (2016).